(15) R. L. Ward and S. I. Weissman, *J. Am. Chem. Soc.*, **79**, 2086 (1957).
(16) N. Hirota in "Radical Ions", E. T. Kaiser and L. Kevan, Ed., Wiley, New York, N.Y., 1968, p. 75.
(17) N. Hirota and S. I. Weissman, *J. Am. Chem. Soc.*, **86**, 2537 (1964).
(18) P. J. Zandstra and S. I. Weissman, *J. Am. Chem. Soc.*, **84**, 4408 (1962).
(19) M. A. Komarynsky and S. I. Weissman, *J. Am. Chem. Soc.*, **97**, 1589 (1975).
(20) T. A. Miller, R. N. Adams, and P. M. Richards, *J. Chem. Phys.*, **44**, 4022 (1966).
(21) R. Chang and C. S. Johnson, *J. Am. Chem. Soc.*, **88**, 2338 (1966).
(22) S. P. Sovensen and W. H. Bruning, *J. Am. Chem. Soc.*, **95**, 2445 (1973).
(23) M. A. Komarynsky and A. C. Wahl, *J. Phys. Chem.*, **79**, 695 (1975).
(24) Y. Shimozato, K. Shimada, and M. Szwarc, *J. Am. Chem. Soc.*, **97**, 5831 (1975).
(25) T. Layloff, T. Miller, R. N. Adams, H. Fäh, A. Horsfield, and W. Proctor, *Nature (London)*, **205**, 382 (1965).
(26) D. Behar and R. W. Fessenden, *J. Phys. Chem.*, **75**, 2752 (1971).
(27) L. K. Patterson and J. Lilie, *Int. J. Radiat. Phys. Chem.*, **6**, 129 (1974).
(28) R. H. Schuler and G. K. Buzzard, *Int. J. Radiat. Phys. Chem.*, in press.
(29) B. Venkataraman, B. G. Segal, and G. Fraenkel, *J. Chem. Phys.*, **30**, 1006 (1959).
(30) M. E. Peover, *Electrochim. Acta*, **13**, 1083 (1968).

Transmission of Substituent Effects. Generalization of the Ellipsoidal Cavity Field Effect Model[1]

S. Ehrenson

Contribution from the Chemistry Department, Brookhaven National Laboratory, Upton, New York 11973.

Received May 24, 1976

Abstract: The ellipsoidal cavity field effect model of Westheimer and Kirkwood for transmission of polar substituent effects is extended to remove the constraint of interacting site-focus coincidence. This allows more rational specification of the geometry of the cavity, and hence of the effective dielectric, based upon physically realistic intermolecular (solute-solvent) distances. Significant improvements in the power of the model are noted upon application to several experimentally studied systems, both in terms of the quality of relative reactivity predictions and in internal self-consistency.

One crucial constraint imposed on the ellipsoidal cavity field effect model[2] for transmission of polar substituent effects upon reactivity seriously hampers evaluation of the model's true merit.[3] This involves location of the interacting sites at the foci of the ellipsoid of revolution which, together with specification of the cavity volume or "imbedding" factor, completely determines the size and shape of the cavity, often completely unrealistically. That any doubt presently exists concerning the superiority of the field over the classical inductive (bond falloff) model[8] is likely due to this condition and how it can in fact *impede* operational improvement of known deficient spherical cavity representations.

What is suggested here is that more directly relevant geometrical information be used in determination of the cavity dimensions. For molecules having axial symmetry with interacting sites located at terminal molecular positions along the axis, as is often the case, at least upon intramolecular rotational averaging, the "imbedding" distance of these sites is usefully retained. It is, however, to be a reasonable physical distance, rather than an empirical value generated from other closely related systems.[13] If the partial molar volume is well known and relatable to cavity volume, it should of course be used. If not, one other internal site to cavity-edge distance, preferably involving a framework locus, would uniquely define the cavity dimensions.

Such physically reasonable ellipsoidal cavities do not conform to the requirement of focus-interacting site coincidence. In fact, for most molecules of interest, particularly those with rigid framework where precise knowledge of geometry is possible, the interacting sites are often predicted to lie significantly away from the foci. To accommodate such cases, partial rederivation of the Westheimer and Kirkwood (WK) electrostatic work equations are necessary and are as follows.

Laplace's equation in prolate spheroidal coordinates for an axially symmetric potential, ψ, is

$$\frac{\partial}{\partial\lambda}(\lambda^2 - 1)\frac{\partial\psi}{\partial\lambda} + \frac{\partial}{\partial\mu}(1 - \mu^2)\frac{\partial\psi}{\partial\mu} = 0 \qquad (1)$$

where $\lambda = (r_1 + r_2)/R$, $\mu = (r_1 - r_2)/R$, r_1 and r_2 are the distances of a point from the ellipsoid foci and R is the interfocal distance. As before,[2] the potential inside and outside the cavity fulfilling eq 1 are

$$\psi_{\text{in}} = D_{\text{i}}^{-1} \sum_{\substack{\text{charges}\\ k}} \frac{e_k}{|r - r_k|} + \sum_{n=0}^{\infty} B_n P_n(\mu) P_n(\lambda) \qquad (2)$$

$$\psi_{\text{ex}} = \sum_{n=0}^{\infty} A_n P_n(\mu) Q_n(\lambda) \qquad (3)$$

and the boundary conditions are

$$\psi_{\text{in}}(\lambda_0,\mu) = \psi_{\text{ex}}(\lambda_0,\mu)$$

$$D_{\text{i}}\left(\frac{\partial\psi_{\text{in}}}{\partial\lambda}\right)_{\lambda=\lambda_0} = D_{\text{s}}\left(\frac{\partial\psi_{\text{ex}}}{\partial\lambda}\right)_{\lambda=\lambda_0} \qquad (4)$$

where D_{i} and D_{s} are the dielectric constants inside and outside (solvent) of the cavity, both regions considered continuous (structureless), λ_0 defines the boundary ellipsoid with μ ($1 \geq \mu \geq -1$), and P_n and Q_n are, respectively, the nth order Legendre polynomials of the first and second kind.

It is at this point that the WK derivation is generalized. To match the boundary conditions, $|r - r_k|^{-1}$ is expanded by the generalized Neumann relationship,[15] valid for e_k located anywhere on the major axis,[16]

$$|r - r_k|^{-1} = R^{-1} \sum_{n=0}^{\infty} 2(2n + 1) P_n(\lambda_k) P_n(\mu_k) Q_n(\lambda) P_n(\mu) \qquad (5)$$

Following solution for B_n, as in ref 2, the difference in electrostatic work for the compared processes may be computed.

For interaction of two poles located symmetrically away from the foci, i.e., in symmetric dibasic acid ionizations,[18]

$$\Delta W = 2.303kT\Delta pK = e^2/\rho D_{\text{e}} \qquad (6)$$

$$D_{\text{i}}/D_{\text{e}} = \left\{1 + 2\xi[(D_{\text{i}}/D_{\text{s}}) - 1] \sum_{n=0}^{\infty} \frac{P_n^{\,2}(\xi) U_n}{1 - (D_{\text{i}}/D_{\text{s}}) C_n}\right\} \qquad (7)$$

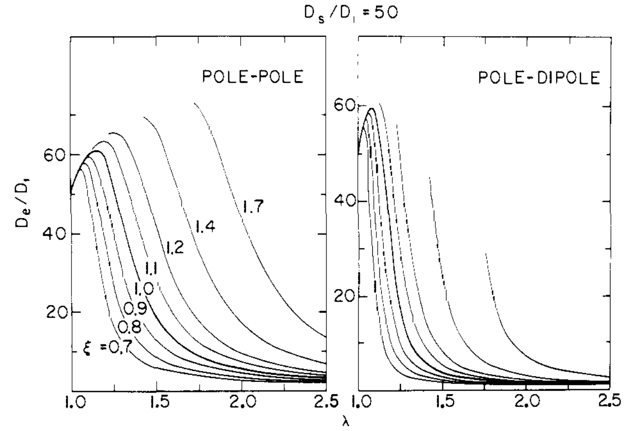

Figure 1. D_e/D_i vs. λ for the generalized pole-pole and pole-dipole electrostatic interaction models with $D_s/D_i = 50$.

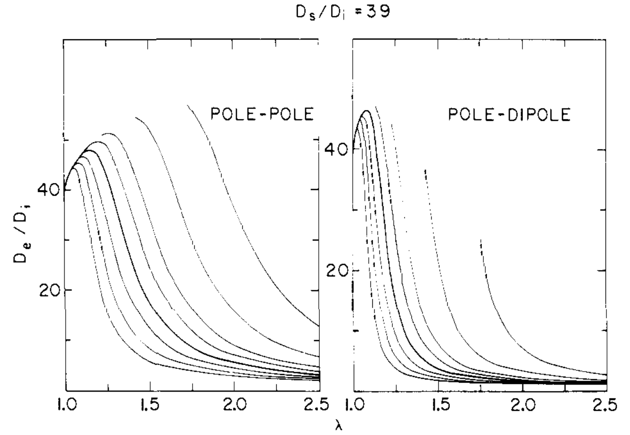

Figure 2. D_e/D_i vs. λ for the generalized pole-pole and pole-dipole electrostatic interaction models with $D_s/D_i = 39$. The individual curves appear in the same order here and following as in Figure 1 where their ξ dependence is explicitly labeled.

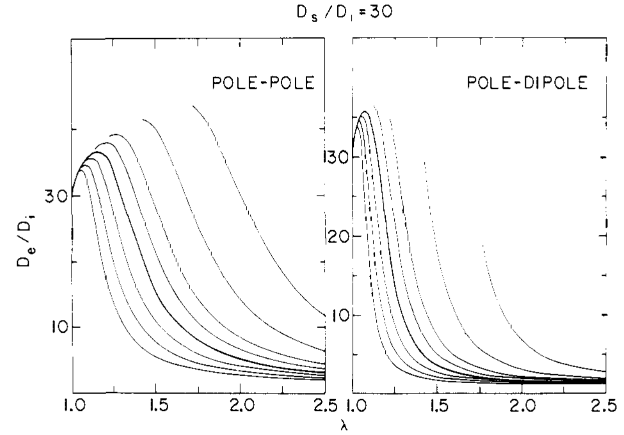

Figure 3. D_e/D_i vs. λ for the generalized pole-pole and pole-dipole electrostatic interaction models with $D_s/D_i = 30$.

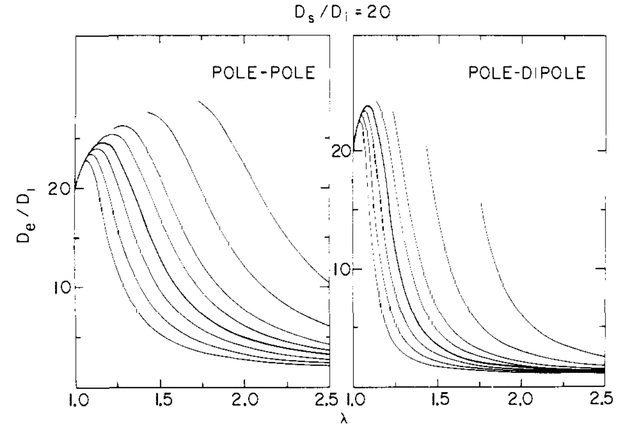

Figure 4. D_e/D_i vs. λ for the generalized pole-pole and pole-dipole electrostatic interaction models with $D_s/D_i = 20$.

where ρ is the interacting site distance, $\xi = \rho/R$, U_n and C_n are as in ref 2,[19] and D_e, the effective dielectric experienced by the interacting sites, is the central quantity of interest.

$$U_n = (2n + 1)(-1)^n[Q_n(\lambda_0/P_n(\lambda_0)] \tag{8}$$

$$C_n = \frac{\lambda_0 - (P_{n-1}(\lambda_0)/P_n(\lambda_0))}{\lambda_0 - (Q_{n-1}(\lambda_0)/Q_n(\lambda_0))} \tag{9}$$

In similar fashion for pole-point dipole interaction, both located symmetrically with respect to the foci,

$$\Delta W = 2.303kT \log K'/K = e\mu \cos \theta/\rho^2 D_e \tag{10}$$

where μ is the bond moment of the substituent (the primed system) relative to the standard, and ρ and θ are, respectively, the interacting site distance and angle formed by the vector ρ and the substituent dipole, assumed identical in the compared systems.[21] Here

$$D_i/D_e = \left\{1 + 4\xi^2[(D_i/D_s) - 1] \sum_{n=0}^{\infty} \frac{nY_n}{1 - (D_i/D_s)C_n}\right\} \tag{11}$$

with

$$Y_n = U_n \left\{\frac{\xi P_n(\xi) - P_{n-1}(\xi)}{1 - \xi^2}\right\} \tag{12}$$

and all other symbols are as before.

While reasons for originally constraining the interacting sites to the foci can only be conjectured, examination of eq 7 and 11 reveal difficulties which would have been encountered if this constraint were relaxed. The infinite sums are quickly seen to be more slowly convergent with increased ξ, and loss of numerical significance in upward recurrence for $Q_n(\lambda_0)$, as employed in ref 2, would preclude accurate evaluation of D_e. Further details in the derivation of eq 7 and 11 and an alternative procedure for evaluation of the Q_n in terms of hypergeometric functions which avoid this convergence problem are briefly outlined in the Appendix.

Figures 1-4 contain the variations of D_e/D_i with λ_0, families of curves over ξ, for both the pole-pole and pole-dipole cases. A useful range of the parameter D_s/D_i is considered.[23] Preceding application to several examples, it is useful to note the considerable effect movement of the interacting sites with respect to foci can have, particularly in the pole-dipole cases when the cavity is highly eccentric. Note, as well, $\xi \le \lambda_0$; when equal, the sites are located at the cavity surface.

In Table I results pertaining to the pK_a difference of bicyclo[2.2.2]octanedicarboxylic acid are presented for several field models. The experimental value of log $(K_1/4K_2)$ and structural data for the acid are from ref 10. It is immediately apparent that the original WK model fails rather badly in rationalizing the ΔpK_a, to a large extent because of the not-surprising failure of Traube's rule (see column 2, Table I). The deficiency in molar volume estimation by this rule for geometrically simpler systems has been previously noted;[7] the underestimation is of course worse for bicyclo systems where significant solvent exclusion is to be expected. The too-small Traube cavity volume is reflected in unrealistic reactant to cavity-edge distances, particularly in the repulsive interaction distance δ (see Table I footnotes for description). Based on van der Waals radii, this distance should be well over 2 Å. Similarly, but not as extreme

Table I. ΔpK_a of Bicyclo[2.2.2]octanedecarboxylic Acid[a]

		Ellipsoidal models			
	Spherical model	$\xi = \mathbf{1.0}$			
		Traube[b]	H bond[c]	D_e expt[d]	$\xi = 1.14$[e]
V (ml/M)	371	**160**	240	281	303
d (Å)	**1.0**	1.2	**1.6**	1.8	**1.6**
δ (Å)	2.9	1.0	1.7	1.9	**2.6**
e	0.00	0.78	0.73	0.71	0.64
D_e	40	51	43	**37**	37
$\log K_1/4K_2$	0.71	0.55	0.67	**0.77**	0.77

[a] Experimental and some other data for previously considered models from ref. 10a, Table V; $D_s = 50$ for 50% (weight) corresponding to 50% (weight) ethanol in water at 25 °C. The structural parameters displayed are in row order: V, the volume of the cavity; d, the distance along the major axis from the ionizable proton position to the cavity edge; δ, the distance along the bisector of the framework CH_2 from the H projection position to the cavity edge; e, the eccentricity of the ellipse; D_e, the effective dielectric constant experienced in the ionization process; and the appropriate ΔpK_a measure conforming to eq 6. The boldface entries are input and/or constraints. D_i, here and elsewhere, = 2. [b] The Traube's rule partial molar volume. [c] Input hydrogen bonding distance (to O) for ionizable protons. [d] WK cavity which would produce the experimental ΔpK. [e] Input H bonding and van der Waals (H-O) framework repulsion distances.

Table II. Log K_X/K_H for 4-Substituted Bicyclo[2.2.2]oct-2-ene-1-carboxylic Acids[a]

	Spherical	Ellipsoidal models			
Group	model[b]	$\xi = 1.0$[d]	d, δ[e]	d, δ[f]	Expt
H[c]	(0.12)	(0.07)	(0.13)	(0.14)	
CH_3	−0.04	−0.04	−0.03	−0.03	0.04
CF_3	0.37	0.19	0.53	0.61	0.76
Cl	0.53	0.31	0.54	0.55	0.83
CN	0.60	0.19	0.74	0.88	1.05
$N(CH_3)_3^+$[g]	1.52		1.51	1.80	1.71

[a] From ref. 10a, Table V, all data except columns 3 and 4; $D_s = 50$, for 50% (weight) ethanol in water at 25 °C. [b] Tanford imbedding factor, $d = 1.0$ Å. [c] Values in parentheses for 4-H derivative relative to hypothetical acid of same size and shape, but without dipolar group, see ref 21. [d] Employing the Traube's rule partial molar volumes. [e] Average d and hence ξ from H bonding (1.6 Å) at acid end and van der Waals repulsion along major axis at the other. δ assumed the same as in Table I calculations. Center of dipole at middistance from C_4 to substituent end projection on major axis. [f] Same as footnote e except ξ as the geometric mean, $\sqrt{\xi_1 \xi_2}$, where the ξ's are the distances from the ellipsoid center to the interacting sites, normalized to half the interfocal distance. This averaging may under certain circumstances be slightly superior for single ξ determination of D_e for asymmetric systems (see the Appendix). [g] From eq 6 with appropriate H group reference.

is the close approach required for solvent to the ionizable proton, as measured by d.

If one employs a reasonable hydrogen-bonding distance for d, retaining the focus-interacting site constraint, the results in the third column are obtained. These, while significantly better in all respects, still imply an overly short δ, i.e., that too many of the lines of force go through the high dielectric solvent medium. It is interesting at this point to examine the spherical cavity results (column 1). Here, following the Tanford prescription ($d = 1.0$ Å), a quite good ΔpK_a result is obtained. The physically unrealistic d value is obviously compensated for by the also unrealistic δ value in the other direction. The very large cavity volume required in this model is to be noted as well.

In column 4, dimensions of the WK cavity necessary to reproduce the experimental ΔpK are displayed. Here, d is almost a correct H-bonding distance but, again, the repulsion distance is small. Clearly, the constrained ellipsoids are too eccentric to properly accommodate the reactant.

Relaxing the focus-interacting site correspondence constraint allows the acid to be properly fit within the cavity. The results of the last column indicate the obvious improvements which accompany this generalization. Here, where the distances d and δ are the sole input, the ionizable protons are predicted to lie significantly outside the foci ($\xi = 1.14$), the cavity is somewhat more nearly spherical ($e = 0.64$), and the computed and experimental $\log K_1/4K_2$ values are, perhaps astonishingly considering the approximations still contained in the model, found to be exactly the same.

Application of the generalized model to substituent constant effects in similar bicyclo systems is also found to result in substantial improvements. Table II presents results for ionizations of the simpler 4-substituted bicyclo[2.2.2]oct-2-ene-1-carboxylic acids, data also obtained by Stock et al.[10] Here, again, of simple shapes, unconstrained elliptical cavities appear physically most appropriate; considerably greater approximations are necessary to accommodate the reactant therein and to define plausible geometries, however. The footnotes of the table describe the procedures employed. Conceptually, the dissymmetry of the molecule as regards the interacting sites is most relevant. Assuming an average symmetrical configuration about the foci follows similar assumptions made previously in application of field effect models.

In all cases, the generalized approach employing reactant to cavity-edge interaction distances is seen to be much more effective in reproducing the experimental acidities than the Traube volume model, and, although less dramatically, better as well than the spherical cavity model which again exaggerates the molar volumes and repulsive interaction distances. In contrast to the ΔpK_a studies, here, with the exception of X = H, all cases are characterized by interacting sites lying inside the foci ($\xi < 1$, often as low as 0.75). The $\log K_X/K_H$ values remain consistently low compared to experiment, most likely because of the assumptions made concerning the substituents as point dipoles (principally of their positions and postulated noninteraction with the molecular framework). Considerable speculation concerning these and related matters appears regularly among the references cited and will not be rehashed here; suffice it to say that the corrections they lead to are much less needed upon application of the extended, more physically rational ellipsoidal cavity model.

As a final example, the ΔpK_a values of the straight-chain aliphatic ω-dicarboxylic acids are computed employing the extended model. Results obtained are presented in Table III along with the experimental values of Peek and Hill[24] and those forthcoming from the original WK model using Traube's rule. The point of major interest here are the interaction distances between the acid proton sites connected by flexible frameworks.

Defining the cavities through reasonable estimations of acid-cavity-edge distances (see footnote b of Table III) yields ξ values quite near to unity. These are slightly higher than one for the smaller acids, rapidly converging to values slightly smaller (~0.93) with increased acid size and slightly larger for the free rotation than extended configurations. It is not surprising, therefore, that the original and extended models are found to produce similar results, particularly for the longer chain species. For the latter, compensation between λ and ξ produces similar D_e values for both models. In the smaller molecules, succinic acid in particular, the extended model requires a considerably larger λ (relative to the original model), more than the ξ difference can compensate for, producing a smaller relative D_e and, hence, a greater ΔpK_a for either choice of ρ.[25]

Table III. ΔpK_a of Aliphatic ω-Dicarboxylic Acids[a]

Acid	ξ = 1.0, Traube volume		d, δ[b]		
	FR R	Max R	FR R	Max R	Expt
Succinic	1.26	0.54	2.23	1.04	0.91
Glutaric	1.11	0.47	1.74	0.68	0.52
Adipic	0.96	0.32	1.37	0.41	0.37
Pimelic	0.88	0.29	1.12	0.34	0.32
Suberic	0.80	0.25	0.94	0.26	
Azelaic	0.73	0.23	0.80	0.24	0.31
Sebacic	0.68	0.21	0.70	0.21	0.30
Dodecanedioic	0.59	0.18	0.54	0.18	0.26
Tetradecanedioic	0.52	0.16	0.45	0.16	0.21

[a] Experimental values for 20% (weight) methanol in water at 25 °C, $D_s = 69$; Traube volumes and free rotation (FR R) and maximum (Max R) interprotonic distances, ρ, from ref 24. ΔpK's from eq 6 and 7. [b] The ellipsoids defined by assuming molecular frameworks lie symmetrically along major axes of length $\rho + 2(r_{HB})$, where r_{HB} is the hydrogen bonding distance to the cavity edge and where the H-projection position of the central CH_2 along its bisector to the cavity edge is the van der Waals distance to oxygen (2.6 Å), see Table I.

The implications of these results, upon comparison with those from experiment, are as follows. In agreement with the Peek and Hill conclusion, the average configurations for the long-chain species appear reasonably to lie between those where free rotation is possible and where maximum extension of the framework is demanded, although considerably closer to the latter. For the smaller acids, assumption of maximum extension produces ΔpK_a values quite close to those observed, whereas free-rotation configuration values are much too high. This, it would seem, is most physically satisfying; the acid proton ends should be maximally separated, particularly upon ionization and notwithstanding the uncertainty in the separation distances incumbent upon averaging over the un-, half-, and completely ionized species in the calculations.

In conclusion, it is apparent that extension of the original elliptical cavity model to allow for more reasonable cavity sizes, shapes, and incorporation of appropriate reactant molecules therein represents a significant improvement over both the original constrained formulation and the more empirical Tanford spherical model. By inference, the electrostatic work concept for rationalization of substituent effects at a distance through nonconducting media is substantially strengthened and, concomitantly, the classical inductive vs. field transmission controversy brought still nearer resolution. Further tests of the ultimate reliability of the extended field model are of course still necessary and are anticipated.

Acknowledgment. The comments of Professors J. Hine and B. M. Wepster on an early draft of this manuscript, particularly in pointing out the existence of ref 20, are gratefully acknowledged. An anonymous referee is also to be thanked for directing the author's attention to the errata, ref 4b, wherein most of the errors of ref 2 are corrected, and which verifies the inferences drawn in the first sentence of ref 19.

Appendix

Generalization of the D_e Equations. For the charge e_k located on the major axis outside the ellipsoidal focus by x, the defining equations for λ and μ in terms of r_1, r_2, and R yield

$$\lambda_{k+} = [x + (R + x)]R^{-1} = \xi$$
$$\lambda_{k-} = [(R + x) + x]R^{-1} = \xi$$
$$\mu_{k+} = [x - (R + x)]R^{-1} = -1$$
$$\mu_{k-} = [(R + x) - x]R^{-1} = 1$$

The + and − signify, respectively, location to the left of the left focus and to the right of the right focus. Recognition that $\rho = R + 2x$, $P_n(1) = 1$, and $P_n(-\xi) = (-1)^n P_n(\xi)$ and substitution into eq 5 following evaluation of B_n yields eq 7.

If the interacting sites are located inside the foci by x, the ellipsoidal parameters are

$$\lambda_{k+}\ [x + (R - x)]R^{-1} = 1$$
$$\lambda_{k-} = [(R - x) + x]R^{-1} = 1$$
$$\mu_{k+} = [x - (R - x)]R^{-1} = -\xi$$
$$\mu_{k-} = [(R - x) - x]R^{-1} = \xi$$

Since $P_n(\lambda_k)P_n(\mu_k)$ is parametrically independent of position inside or outside the focus, the same relationship (eq 7) holds, but, because $\xi < 1$ for location inside the focus, a faster converging series for D_i/D_e pertains.

For the point dipole-pole interaction the following factor must be evaluated

$$2e\mu \cos\theta \lim_{\delta\to 0} \left\{ \frac{1}{\delta} \left[P_n\left(\frac{\rho - \delta}{R}\right) - P_n\left(\frac{\rho + \delta}{R}\right) \right] \right\} \quad \text{(A1)}$$

This may be accomplished through use of L'Hospital's rule, recognizing $(1 - z^2)(dP_n(z)/dz) = n(P_{n-1}(z) - zP_n(z))$. The result is

$$e\mu \cos\theta \left\{ \frac{4n}{R} \left[\frac{\xi P_n(\xi) - P_{n-1}(\xi)}{1 - \xi^2} \right] \right\} \quad \text{(A2)}$$

Generation of the Legendre Polynomials. Upward recurrence of $P_n(z)$ employing $(n + 1)P_{n+1} = (2n + 1)zP_n - nP_{n-1}$ results in very little loss of significant figures and its use in eq 7-12 is justified. For $Q_n(z)$, $z > 1$, however, where the same recurrence relationship holds, the instability is severe; e.g., for $z = 2.6$, starting with nine significant figures for Q_0, only three figures are retained at Q_5.[26a] Note, $Q_0 = \frac{1}{2} \ln [(z + 1)/(z - 1)]$, $Q_1 = zQ_0 - 1$, $P_0 = 1$, and $P_1 = z$.

In order to avoid this, Q_n may be evaluated directly through use of the hypergeometric function,[26b] i.e.,

$$Q_n(z) = \frac{\pi^{1/2}}{(2z)^{n+1}} \frac{\Gamma(n + 1)}{\Gamma(n + 3/2)} F\left(\frac{n}{2} + 1, \frac{n}{2} + \frac{1}{2}, \frac{3}{2} + n, z^{-2}\right) \quad \text{(A3)}$$

or preferably for even more rapid convergence for z close to unity, since

$$F(a,b,c,y) = (1 - y)^{c-a-b}F(c - a, c - b, c, y) \quad \text{(A4)}$$

from

$$Q_n(z) = \frac{\pi^{1/2}}{(zp)^{n+1}} \frac{\Gamma(n + 1)}{\Gamma(n + 3/2)} F\left(n + 1, \frac{1}{2}, n + \frac{3}{2}, \frac{q}{p}\right) \quad \text{(A5)}$$

$$= \frac{1}{(zp)^{n+1}} \sum_{j=0}^{\infty} \frac{\Gamma(n + 1 + j)\Gamma(1/2 + j)}{j!\Gamma(n + 3/2 + j)} \left(\frac{q}{p}\right)^j \quad \text{(A6)}$$

where $q = 1 - \sqrt{1 - z^{-2}}$, $p = 1 + \sqrt{1 - z^{-2}}$, and Γ are the gamma functions.

In practice, rather than generate Q_n for each value of n; the values at index km and $km - 2$ were generated employing eq A6 and *downward* recurrence followed. In this procedure, significance loss is minor; e.g., where $m = 10$, as was usually adopted, loss of two or three figures (of the convergently significant 12 carried on the CDC 7600) was noted typically. The number of repeats (k) is of course determined by the rates of convergence of eq 7 and 11. For extreme λ_0 and ξ ($\lambda_0 \to 1$, $\xi \to \lambda_0$), on the order of 100 terms might be required for convergence in D_i/D_e to one part in 10^6. This convergence behavior, it might be remarked, probably accounts for the decreased significance in reported values (ref 2, Table I and Figure 1) for small λ_0 and the cutoff at $\lambda_0 = 1.1$, high boundary to an interesting region as regards comparative pole and dipole

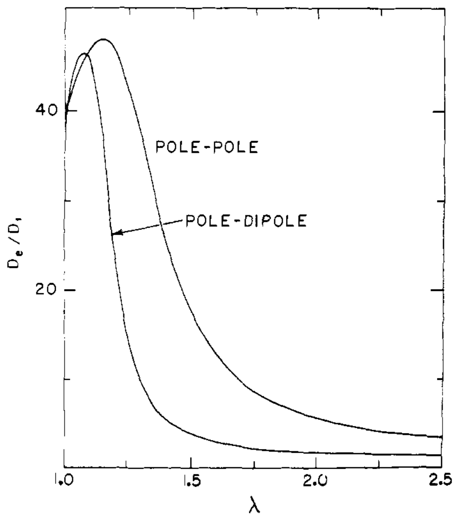

Figure 5. Pole-pole and pole-dipole D_e/D_i vs. λ plots for $D_s/D_i = 39$ and $\xi = 1.0$.

effects. Compare Figure 5, here and, as well, ref 19 and 20.

Averaging for Asymmetric Site Locations. For interacting sites located asymmetrically away from the foci, eq 7 is correctly modified by replacement of $\xi_1 + \xi_2$ for 2ξ as the multiplicative factor of the sum and by $P_n(\xi_1)P_n(\xi_2)$ for $P_n{}^2(\xi)$ within the sum. For systems characterized by large λ_0 and ξ's not too different from unity, where convergence in the sum term is rapid, arithmetic averaging ($\xi = \frac{1}{2}(\xi_1 + \xi_2)$) to return to the original form is an acceptable approximation. Geometric averaging may, however, be preferable as regards stability upon cancellation within the sum term. For example, it may be shown that, whereas the terms within the sum for arithmetic averaging would be in error by factors of 1, $1 + \delta^2$, $1 + 6\delta^2$, and $1 + 21\delta^2$ for $n = 0$–3 with $\delta = (\xi_2 - \xi_1)/2$ assumed small and $\xi \simeq 1$, the corresponding factors upon geometric averaging would be 1, 1, $1 + 3\delta^2$, $1 + 15\delta^2$. However, it should be recognized that the multiplicative factor 2ξ is in error by $1 - \delta^2$ under the latter procedure and correct upon arithmetic averaging.

Useful Cavity Geometry Relationships. Revolution about x (major) axis.

$$V = (\pi/6)R^3(\lambda^3 - \lambda) = (4/3)\pi ab^2$$

$$2a = \text{major axis of ellipse} = \rho + 2d$$

$$2b = \text{minor axis of ellipse}$$

$$R = \sqrt{(2a)^2 - (2b)^2};\ \lambda = 2a/R;\ \xi = \rho/R$$

$$(x/a)^2 + (y/b)^2 = 1$$

References and Notes

(1) Research carried out at Brookhaven National Laboratory under contract with the U.S. Energy Research and Development Administration.

(2) F. H. Westheimer and J. G. Kirkwood, *J. Chem. Phys.*, **6**, 513 (1939).

(3) Generalization from spherical[4] to ellipsoidal cavity shapes for containment of the reaction species represents, it should be recognized, an important conceptual improvement in the model. Both, as extensions of the electrostatic work formulations of Bjerrum[5] and Eucken[6] for multipole interactions *at a distance*, were and continue to be applied predominantly to systems where the molecular framework thickness is considerably less than the interacting site distance. Many of the factors influencing average reactant molecule geometries, upon which specification of these distances depend, have been examined in detail for a variety of systems.[7]

(4) (a) J. G. Kirkwood and F. H. Westheimer, *J. Chem. Phys.*, **6**, 506 (1939); (b) *ibid.*, **7**, 437 (1939).

(5) N. Bjerrum, *Z. Phys. Chem.*, **106**, 219 (1923).

(6) A. Eucken, *Angew. Chem.*, **45**, 203 (1932).

(7) See, e.g., F. H. Westheimer and M. Shookhoff, *J. Am. Chem. Soc.*, **62**, 269 (1940); F. H. Westheimer, W. A. Jones, and R. A. Lad, *J. Chem. Phys.*, **10**, 478 (1942); F. H. Westheimer and J. G. Kirkwood, *Trans. Faraday Soc.*, **43**, 77 (1947).

(8) Analysis of a number of early applications where either classical or field induction could be supported as modes of polar effect transmission revealed the ambiguity to arise mainly because of the limited scope and precision of the data available, notwithstanding the obvious simplifications made in the models such as assumption of continuous media characterized by macroscopic dielectric constants and of bond type independence for falloff.[9] Consequently, recent studies have been undertaken which strongly suggest the classical model to be untenable and, considerably less strongly, the field model to be generally acceptable.[10-12]

(9) S. Ehrenson, *Prog. Phys. Org. Chem.*, **2**, 195 (1964).

(10) (a) F. W. Baker, R. C. Parish, and L. M. Stock, *J. Am. Chem. Soc.*, **89**, 5677 (1967); (b) L. M. Stock, *J. Chem. Educ.*, **49**, 400 (1972).

(11) C. F. Wilcox and C. Leung, *J. Am. Chem. Soc.*, **90**, 336 (1968).

(12) C. L. Liotta, W. F. Fisher, E. L. Slighton, and C. L. Harris, *J. Am. Chem. Soc.*, **94**, 2129 (1972); C. L. Liotta, W. F. Fisher, G. H. Greene, Jr., and B. L. Joyner, *ibid.*, **94**, 4891 (1972).

(13) Tanford,[14] following earlier investigators, sought general empirical imbedding factors for spherical and constrained elliptical cavities. He is responsible for the $d = 1$ Å rule for spherical cavities obtained from ΔpK_a's of dicarboxylic acids, which is often used in field effect calculations on reactivities of all sorts.

(14) C. Tanford, *J. Am. Chem. Soc.*, **79**, 5348 (1957).

(15) Cf., K. Rüdenberg, *J. Chem. Phys.*, **19**, 1459 (1951).

(16) Further generalization to allow e_k to be anywhere within the cavity is possible, but leads to rather complicated, highly parametrized D_e dependences of limited utility. Since many of the cases of interest involve (major) axially symmetric or nearly symmetric systems (upon rotameric averaging), such generalization will not be pursued. Likewise, to maintain simplicity of form, approximate averaging schemes for systems mildly asymmetric about the minor ellipse axis have been employed (vide infra).

(17) J. N. Sarmousakis, *J. Chem. Phys.*, **12**, 277 (1944), has carried out a generalized analysis for oblate spheroidal cavities.

(18) $\Delta pK = \log K_1/\sigma K_2$, where σ is the statistical factor, equal to four for symmetrical dibasic acids.

(19) Several minor errors exist in the ref 2 ΔpK equations, probably arising in transcription, since the figures and tables constructed therefrom appear essentially correct (see however, the Appendix). One of the errors, specifically of sign, appearing in the denominators of the sum terms for both the pole and dipole cases, has unfortunately led to considerable confusion *elsewhere*. Edward et al.,[20] adopting the incorrect formulas, concluded the original WK results were invalid because of unrecognized significance losses in the generation of Q_n. In fact, it is only because of the sign errors that the sums *appear* to converge slowly enough to require more precise generation of Q_n than is provided by upward recurrence (within the WK limits of $\lambda \geq 1.1$, with results to two significant figures). The method for generation of more accurate Q_n outlined in ref 20 is seen to resemble that of the Appendix, making use of hypergeometric functions, but inefficiently (for every n), ignoring the savings of *downward* recurrence. The physical manifestations of this erroneous reanalysis are serious beyond the production of erroneous D_e values (for small λ, <1.7, and increasingly so with increasing eccentricity of the cavity) and should be recognized. The implication that D_e vs. λ relationships need be monotonic suggests that modes of transmission of electrical effects through discontinuous media boundaries of extreme shapes may be simply pictured. Clearly, they cannot always be.

(20) J. T. Edward, P. G. Farrell, and J. L. Job, *J. Chem. Phys.*, **57**, 5251 (1972).

(21) Stock and Holtz[22] have suggested the following modification to account for ρ and θ differences in the substituted and reference reactants:

$$e^{-1}\Delta W = ((\mu \cos\theta)/\rho^2 D_e)_{\text{Prime}} - ((\mu \cos\theta)/\rho^2 D_e)_{\text{Standard}}$$

It would appear that this modification is plausible in the context of the original derivation only when the reactants (and products) are considerably more dissimilar to each other than are the reactant–product pairs. Geometry changes during reaction are uniformly neglected in the electrostatic work derivation.[2,4]

(22) L. M. Stock and H. D. Holtz, *J. Am. Chem. Soc.*, **86**, 5188 (1964).

(23) Limited testing of these figures against generated results for intermediate D_s/D_i and ξ values suggests linear interpolations should suffice for most applications to experimental data. For more precise interpolations, numerical tables from which these plots were constructed are available from the author upon request.

(24) H. M. Peek and T. L. Hill, *J. Am. Chem. Soc.*, **73**, 5304 (1951).

(25) The effective volumes for the short chains are considerably larger in the extended than the original model, whereas in the longer acids they are not very different. There are reasons, following from the model's assumptions of distinct cavity edges through postulation of continuous media, physically meaningless on the microscopic level, which suggest that the real partial molar volume should be somewhat smaller than that obtained upon interaction distance specification. Whether this can account for the apparently general Traube's underestimation of volume is questionable, even for relatively simple molecules not possessing solvent excluding structural details.

(26) (a) See, e.g., M. Abramowitz and I. Stegun, Ed., "Handbook of Mathematical Functions", Dover Publications, New York, N.Y., 1965, p 340; (b) *ibid.*, pp 556–560.